5. Spontaneous and electron-induced adsorption of oxygen on Au(110)-(1×2)

In this chapter, we first study the spontaneous adsorption and condensation of dioxygen on Au(110)-(1×2) at 28 K. We tackle the question of whether oxygen forms chemisorbed species on the gold surface at the very high O_2 surface concentration due to condensation, despite the low temperature (Section 5.1). It proves that Au – unlike most of the other metals including its homologues Cu and Ag – does *not* spontaneously dissociate physisorbed molecular oxygen. Second, we show that activation of the physisorbed O_2 either by electron or by photon impact leads to the formation of chemisorbed atomic oxygen (Section 5.2). This species is extensively discussed in Chapter 6; its reactivity towards CO will be the focus of Chapter 11.

5.1. Physisorbed oxygen

5.1.1. Thermal desorption spectroscopy

DESORPTION STATES AND COVERAGES – Dioxygen[1] was adsorbed at a sample temperature of 28 K using an O_2 partial pressure[2] of 2×10^{-8} mbar for dosing. A representative series of O_2 thermal desorption spectra is displayed in Fig. 5.1. The spectra correspond to initial coverages of ≤ 2.6 ML (exposures ≤ 6.8 L) and were measured with a heating rate of 2.35 K/s.

The desorption states α_3, α_2 and α_1 possess almost coverage-independent temperatures of maximum desorption at 51 K, 45 K, and 37 K, respectively, indicating first-order desorption. We attribute the zero-order peak μ emerging at higher coverages around 34 K to condensed O_2 multilayers. The close vicinity of the peaks μ and α_1 suggests that the latter corresponds to second layer desorption. In agreement with this assignment, the peaks α_3 and α_2 are clearly separated from the multilayer- and the α_1-state, and their combined peak areas are equal to that of the α_1 peak. Accordingly, the desorption states α_3 and α_2 originate from the first adsorbed layer.

Exposure of (2.6 ± 0.5) L afforded monolayer coverage (the error stems from the pressure measurement). The monolayer (ML) is defined here as the maximum number of molecules in direct contact with the surface and corresponds to the combined saturation coverage of the peaks α_3 and α_2. The sticking coefficient of O_2 under the conditions of the experiment was constant, as the coverage dependes linearly on exposure. Dividing the number of desorbed by the number of dosed molecules, as calculated by the collision flux equation, led to a sticking coefficient of 0.5 ± 0.1 for O_2 adsorption on Au(110)-(1×2) at 28 K.

---

[1] Oxygen gas 4.8, purity > 99.998%, Messer Griesheim, Germany.

[2] We divided the meter reading by a factor of 0.8 to account for the different ion gauge sensitivities for N_2 (for which the gauge is calibrated) and O_2.

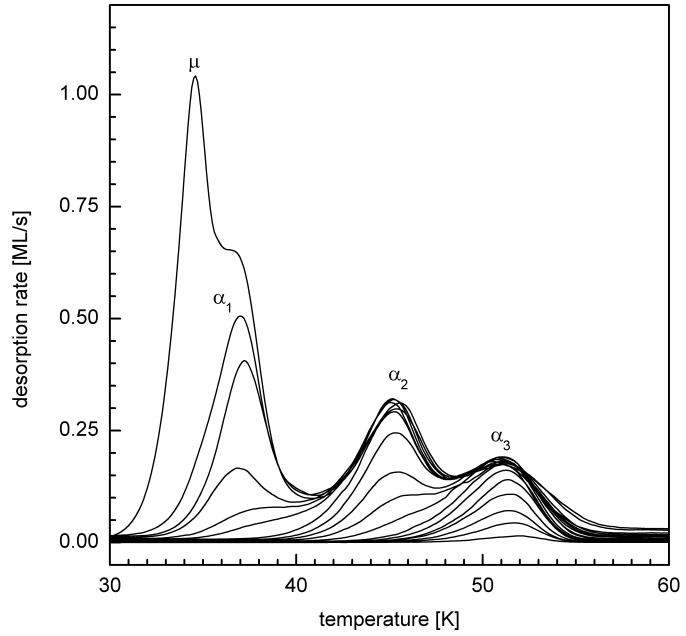

Fig. 5.1. Set of thermal desorption spectra of physisorbed O_2 on Au(110)-(1×2) (detected mass m/z = 32 amu), taken with a heating rate of 2.35 K/s. An exposure of 2.6 L coincides with a coverage of 1.0 ML; the sticking probability was constant for all coverages. The desorption peaks correspond to the following coverages: (α_3) 0.025 – 0.37 ML; (α_2) 0.47 – 0.94 ML; (α_1) 1.08 – 1.78 ML; (μ) 2.60 ML.

The two different desorption states (α_2 and α_3) within the monolayer range might arise from adsorption in sites with higher and lower coordination. The missing-row reconstruction of the Au(110) surface provides such adsorption sites at the bottom (high coordination numbers of 3, 4, or 5) of the trenches and on top of the ridges (low coordination numbers of 1 and 2) between them. Naïvely, one would expect that the higher coordinated molecules possess a higher desorption energy and therefore belong to the α_3 peak. However, physisorbed particles may also prefer sites with low coordination numbers (see, for example, [Na98]). Therefore, the reverse assignment is also possible.

For the monolayer coverage, i.e. for the saturated α_3 and α_2 peaks, an absolute coverage of $(0.51 \pm 0.1)\times10^{19}$ oxygen molecules per m^2 was estimated. With four gold atoms located within the surface unit cell, this coverage corresponds to (0.30 ± 0.06) O_2 molecules per gold atom. Assuming the oxygen molecules have the same packing density on the gold surface as in solid β-O_2 [Hö62], then a coverage of 0.93×10^{19} oxygen molecules per m^2 (corresponding to 0.55 O_2 molecules per gold atom) should be expected. The adsorbed oxygen molecule is apparently larger than that in solid β-O_2, possibly due to polarization effects.

No oxygen desorption was observed above 60 K, excluding the possibility of spontaneous conversion of physisorbed into chemisorbed oxygen on the gold surface. This behaviour differs from that of physisorbed dioxygen on most other metal surfaces, particularly on Ag(110), where physisorbed O_2 is partially converted into chemisorbed dioxygen above 40 K [Pr86].

In addition to these experiments at very high surface concentrations of O_2 and low temperatures we tried to obtain chemisorbed oxygen beyond the O_2 desorption temperature by applying O_2 pressures $\leq 10^{-4}$ mbar for ≤ 600 seconds (corresponding to $\leq 4.6\times10^5$ L) at various sample temperatures up to 700 K. However, no oxygen adsorption occurred under these conditions. This result is consistent with earlier reports on this subject [Ca84, Sa86]. It also confirms the absence of impurities as Ca, Si, and Mg on our sample, since these contaminants are known to catalyse the dissociation of dioxygen on gold.

DESORPTION KINETICS, ACTIVATION ENERGIES, AND FREQUENCY FACTORS – The evaluation of kinetic and energetic parameters from the desorption spectra in Fig. 5.1 bases on the Polanyi-Wigner equation (Eq. 4.1). In order to evaluate the desorption activation energy, E_{des}, and the frequency factor, ν_n, as functions of coverage, the TD spectra were analysed using the well-known leading edge analysis [Ha84]. As described in Section 4.1.3, this method uses the initial part of each TD spectrum, where the *relative* change in coverage is small. Here, the loss of coverage was limited to 5 % of the initial coverage.

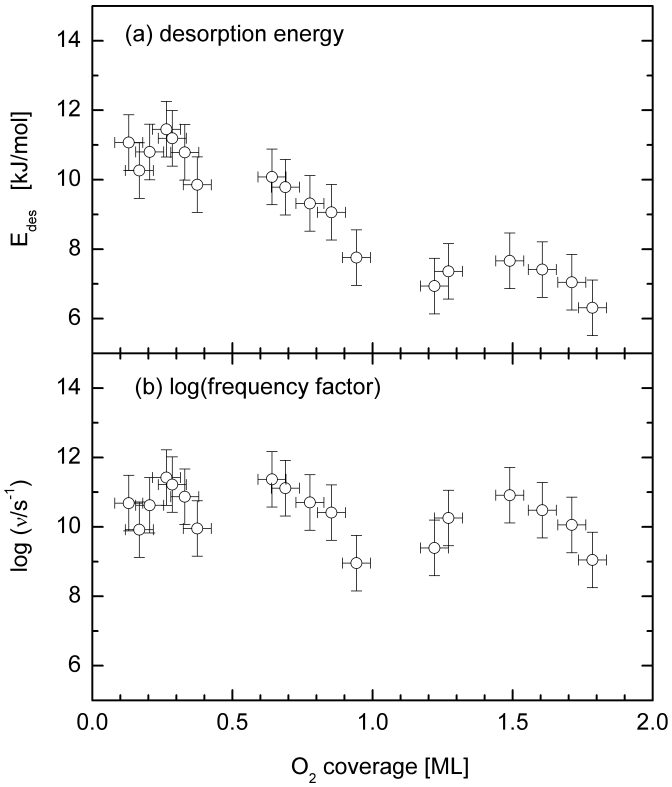

Fig. 5.2. (a) Desorption activation energy and (b) log(frequency factor) for the TD spectra in Fig. 5.1, obtained by leading edge analysis [Ha84].

The results for the spectra of Fig. 5.1 are presented in Fig. 5.2. For the α_3 state (< 0.40 ML), the desorption energy remains at a constant level of $E_{des} \approx 11$ kJ/mol. The frequency factor of $\nu \approx 10^{11}\ s^{-1}$ is slightly lower than the universal frequency factor kT/h, which amounts to $10^{12}\ s^{-1}$ at 51 K. A low frequency factor reflects, within the framework of transition state theory (see Section 3.1, especially Eq. 3.8), a small ratio between the partition functions of transition state and ground state. Thus, either the partition function of the ground state is large, or that of the transition state is small, or both. In the first case, we have a mobile oxygen adlayer with two translational degrees of freedom at the desorption temperature. In the second case, the activated complex is still confined to the surface and the translational, rotational, and vibrational degrees of freedom are not fully excited.

In the coverage range $0.5 < \Theta < 1.0$ ML (α_2 state), the desorption energy E_{des} decreases from 10 to 8 kJ/mol, indicating repulsive interactions between the oxygen molecules even within the submonolayer range. The decrease in the desorption energy parallels a decrease in the frequency factor especially for the α_2 state, suggesting operation of a compensation effect (for a discussion of this effect, see Section 4.1.5).

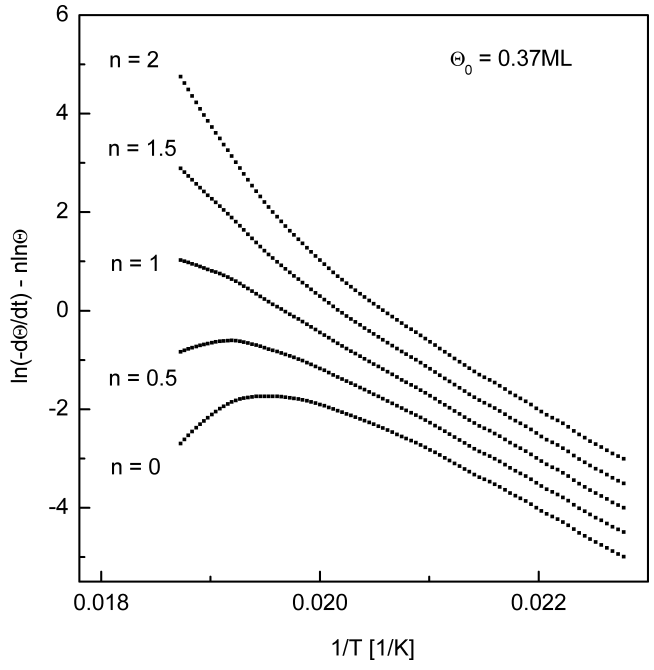

Fig. 5.3. Arrhenius plots for the TD spectrum of an initial coverage of 0.37 ML (α_3 state) in Fig. 5.1. For the choice n = 1 (first-order desorption) a straight line and the following desorption activation parameters were obtained: $E_{des} = 10.7$ kJ/mol, $\nu_1 = 9\times10^{10}\ s^{-1}$.

The activation parameters for the α_3 state are constant within the limits of their error bars. This allows an Arrhenius plot analysis ([Jo90, Pa90] and Section 4.1.3) as shown in Fig. 5.3 to confirm the desorption order n = 1. According to Eq. 4.14, $\ln(R_{des}/\Theta^n)$ was plotted vs. 1/T for different desorption orders n. A (nearly) straight line is only obtained for n = 1, whereas the other curves exhibit the predicted deviations from linearity for incorrect values of n. From the slope and the intercept of a linear fit, mean values of the first-order desorption energy and frequency factor were found to be E_{des} = (10.7±0.5) kJ/mol and $\nu_1 = 9\times10^{10\pm0.5}\ s^{-1}$, respectively, both of which are in good agreement with the results of the leading edge analysis. It should be emphasized this is the first time that oxygen physisorption has been studied without parallel dissociation and chemisorption, i.e., we are reporting the first desorption energy values for oxygen physisorption on a *clean* metal surface.

substrate	Ref.	multilayer O_2	2nd layer physisorbed O_2	physisorbed O_2 on a chemisorbed O layer	physisorbed O_2	chemisorbed O_2
Pt(111)	[Ar96]	9.1* 5×10^{14}	9.0* 1×10^{15}	10.4* 1×10^{12}	-	-
Pt(111)	[Lu89]	-	8*?	11.6*§	-	(34)
Pt(111)	[Gl80]	-	-	-	-	37±2†
W(100) W(110) W(112)	[Le76] [Ch89]	≈7*	≈8*	≈13*	-	-
W(111)	[Os97]	≈7*#	≈8*#	16.4*#	-	-
Ru(10-10)	[Sc02]	8.2	-	14	-	-
Au(110)-(1×2)	this work and [Go02]	8.9 $\equiv \Delta H_{sub}^{corr}$ 1.5×10^{14}	7 (α_1) 3×10^{10} (α_1)	16	8 – 10 (α_2) 10^9 - 10^{11} (α_2) 11 (α_3) 10^{11} (α_3)	-

Table 5.1: Comparison of desorption energies (kJ/mol) and frequency factors (s^{-1}) for O_2/Au(110)-(1×2) with those for some other O_2 physisorption systems. In our work, the multilayer desorption energy was employed for temperature calibration (as described in Section 4.1.2) and is therefore no independently confirmed value (ΔH_S^{corr} stands for corrected sublimation enthalpy). The literature values marked with * were originally reported in eV. The values marked with # were derived in the original work by assuming an average lifetime of 1 second at the desorption temperature. § Assumed frequency factor $10^{13}\ s^{-1}$. In brackets: values estimated from reported TDS data after Redhead [Re62] assuming $\nu = 10^{13}\ s^{-1}$. † Isosteric heat of adsorption.

The desorption energy of physisorbed O_2 on Au(110)-(1×2) agrees with (or is lower than) the respective values for O_2 physisorption on other metal surfaces, confirming the absence of chemisorptive bonding contributions. However, comparison to other metals is obstructed by the fact that oxygen physisorption on *clean* metal surfaces is usually impossible to study by TDS, since physisorbed oxygen is always partially converted into *chemisorbed* oxygen, even well below the desorption temperature of the physisorbed species. To the best of our knowledge, there have been no reports about unperturbed O_2 physisorption at the desorption temperature of physisorbed oxygen (> 30 K). The chemisorbed oxygen adlayer leads to an increased desorption energy of the physisorbed oxygen. We show in Section 5.2.2 that preadsorption of atomically chemisorbed oxygen on the Au(110)-(1×2) surface causes a high-temperature shift of the α_3 peak from 51 K on the clean gold surface to 65 K. This shift explains why our value is lower than most of the respective literature values collected in Table 5.1.

Very close to our results, physisorbed dioxygen on Pt(111), which was partially covered with chemisorbed O or O_2, has a desorption energy of 11.6 kJ/mol [Lu89]. The respective value for chemisorbed O_2 on this surface is much higher, viz., 37 kJ/mol [Gl80]. For chemisorbed dioxygen on Ag(110), Barteau and Madix [Ba80] found a desorption energy in the range 20 - 30 kJ/mol. Tungsten surfaces provide further examples of a superposition of oxygen physisorption and chemisorption: on W(111), dissociative adsorption occurs even at temperatures as low as 5 K [Os97]. Low-temperature oxygen adsorption on the tungsten surfaces (100), (110), and (112) [Le76, Ch89] led in all cases to almost identical desorption patterns consisting of three low-temperature states with estimated desorption energies of 7, 8, and 13 kJ/mol, respectively. These peaks were attributed to condensed (fourth layer), physisorbed (third layer), and weakly chemisorbed (second layer) dioxygen. The first layer was filled with chemisorbed oxygen atoms which desorb around 2100 K. On O/W(111), the second layer had a desorption energy of 16.4 kJ/mol [Os97]. In his excellent study of oxygen adsorption on O/Ru($10\bar{1}0$) at 30 K, Schmidt observed two low-temperature states with desorption energies of 14 kJ/mol (second layer) and 8.2 kJ/mol (condensed O_2) [Sc02].

5.1.2. UV photoelectron spectroscopy

A series of UV photoelectron spectra for increasing O_2 coverages on Au(110)-(1×2) at 28 K is displayed in Fig. 5.4; the corresponding difference spectra can be found in Fig. 5.5. The spectra were measured with synchrotron radiation of 24 eV photon energy in M polarization and normal emission[3]. A low beam intensity combined with short measurement times (20 seconds per spectrum) was applied in order to avoid beam damage which leads to the formation of chemisorbed oxygen[4]. The latter influences the work

[3] For details concerning the geometry of our ARUPS experiment cf. Section 4.2.2.

[4] See Section 5.4.

function of the substrate[5] and, thereby, also the positions of all oxygen-induced signals relative to E_F, as shown in Section 5.2.3. Therefore, any beam damage has carefully to be avoided. In order to prevent the accumulation of the chemisorbed species, the sample was heated to 640 K after each exposure of the adsorbate to synchrotron radiation, a temperature that is sufficient for the complete desorption of chemisorbed oxygen as demonstrated in Chapter 6.

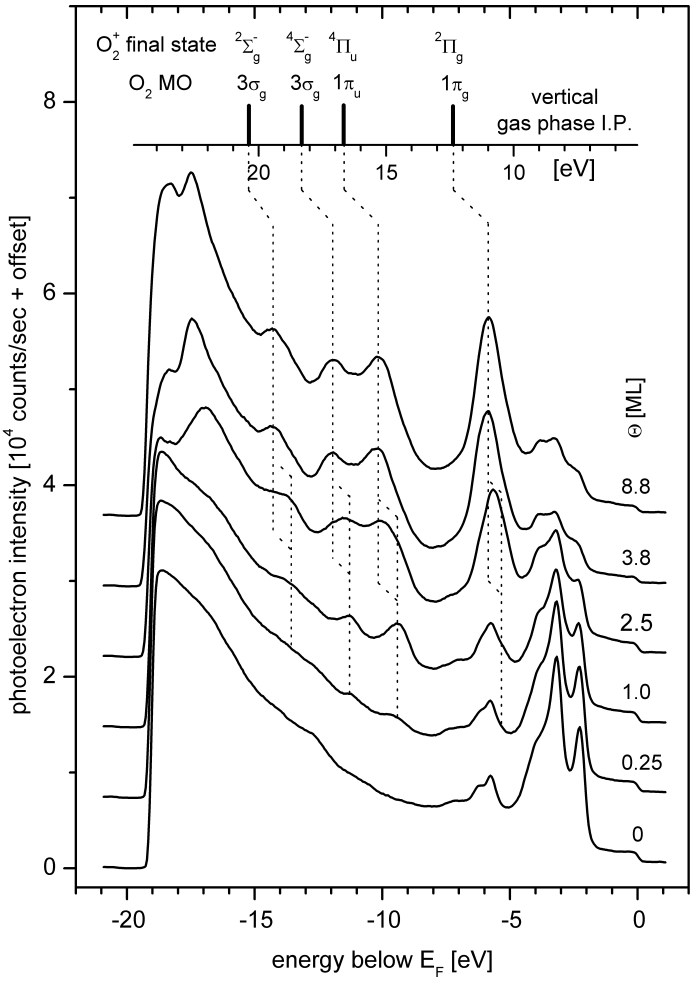

Fig. 5.4. UV photoelectron spectra (hν = 24 eV) of physisorbed dioxygen on Au(110)-(1×2). An exposure of 2.6 L coincided with monolayer coverage. The UV light beam was p polarized with respect to the $(00\bar{1})$ mirror plane and had an incidence angle of $\vartheta_i = 45°$ (polar) and $\phi_i = 0°$ (azimuthal) (cf. Section 4.2.2). The projection of the beam onto the surface was parallel to the $[\bar{1}10]$ direction, i.e., to the trenches on the surface. The photoelectrons were detected in normal emission ($\phi = 0°$). Gas phase values were taken from Ref. [Tu70]. Alignment of the energy scales by shifting the gas phase ionization potentials (after Ref. [Tu70]) by $\varphi + \Delta\varphi$. Potential on the sample –10 V for the reasons described in Section 4.3.4. See text for the further details.

[5] See Section 6.6.

The UP spectra exhibit, over the whole coverage range (0.25 – 8.8 ML), the typical signals of physisorbed oxygen. The close resemblance to the O_2 gas phase UP spectrum in Ref. [Tu70] (apart from the vibrational fine structure) indicates molecular adsorption and allows the assignment of the peaks to the O_2 molecular orbitals and to the final states of the molecular ion, O_2^+. The energetic spacing of the peaks is roughly the same as in the gas phase, i.e., the orbital interactions between O_2 and the metal are weak, in agreement with the low desorption energy of only 11 kJ/mol. A closer inspection of the peak positions, however, reveals small differential shifts within the submonolayer range and (larger) uniform shifts between submonolayer range, multilayer range, and gas phase. The respective data are collected in Table 5.2.

As an example, we discuss the energy differences between the monolayer (Θ = 1.0 ML) and a multilayer spectrum (Θ = 8.8 ML). The respective values, as shown in the bottom line of Table 5.2, contain initial and final state contributions[6]. The major final state effect is a change of the (extra-molecular) relaxation energy, E_{rel}, due to the different screening of the hole in the photoionized oxygen. According to Chiang et al. [Ch86], the screening by the substrate (metallic screening) is more effective than that by a matrix of other O_2 molecules in condensed oxygen (dielectric screening), i.e., E_{rel} should be higher for the molecules which have direct contact to the surface. Since E_{rel} is added to E_{kin}, this effect leads to higher kinetic energies, or lower binding energies, in the monolayer spectrum. On the other hand, binding orbital interactions[7], which would increase the electron binding energy of the involved occupied molecular orbitals of O_2, should result in opposite peak shifts, since the intermolecular orbital interactions between the O_2 molecules are certainly weaker than those between molecule and surface. The observed total shift to *higher* electron binding energies in the multilayer spectrum shows that the final state contribution (i.e., the contribution of the relaxation energy) dominates, or, in terms of Eq. 4.38, $|\Delta(\Delta E_{final})| > |\Delta(\Delta E_{initial})|$. The amount of shift may vary for the particular peaks, as in the case of the $1\pi_g$ level. However, we are not able derive information about certain binding MO interactions from this fact, because it is impossible to disentangle initial and final state contributions, both of which may change differently for each level.

[6] For a general discussion of the energy changes due to the presence of the surface see Section 4.2.1. An additional contribution to the peak shift is the work function difference between the clean surface and a complete O_2 monolayer, i.e., the different work functions 'seen' by a molecule in the first and in the second layer. This contribution amounts here to ≈ 0.2 eV and results in a shift to higher electron binding energies for coverages above 1.0 ML. In the following qualitative discussion we tacitly ignore this contribution.

[7] I.e., chemisorptive contributions to the adsorbate-substrate interaction.

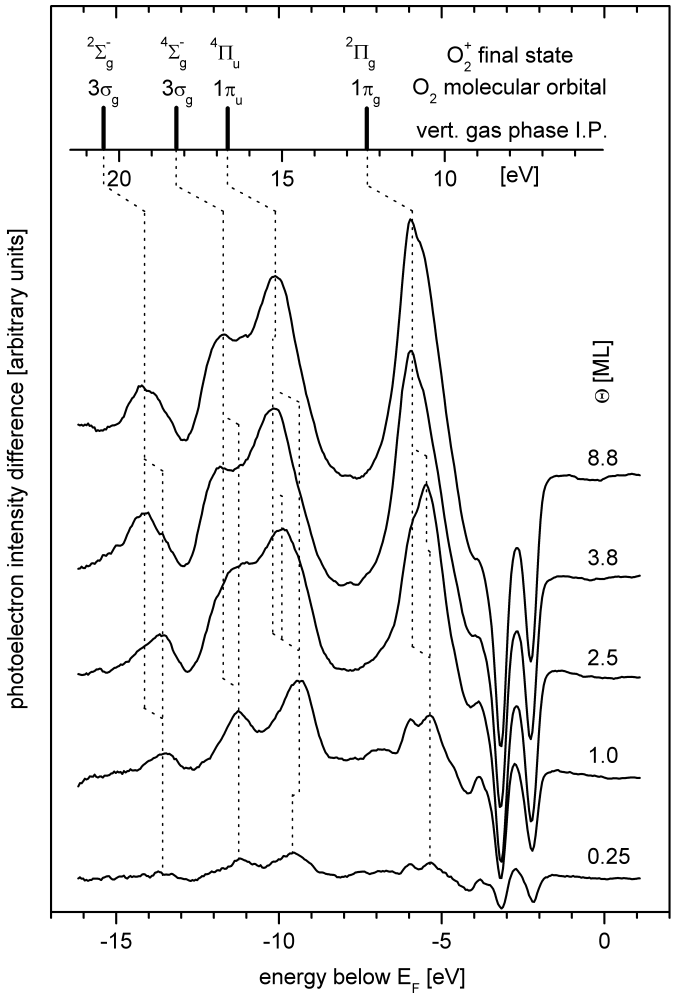

Fig. 5.5. UP difference spectra (hν = 24 eV) of physisorbed dioxygen on Au(110)-(1×2), obtained by subtraction of a spectrum of the clean surface, measured at 28 K, from the spectra in Fig. 5.4. See Fig. 5.4 and the text for the further details.

Comparison of the $1\pi_u$ derived emission in the UP spectra for 0.25 ML and 1.0 ML reveals a peak shift by ≈ 0.2 eV towards lower binding energies with increasing coverage. The 0.25 ML spectrum corresponds to the α_3 desorption state in Fig. 5.1, which has, according to Fig. 5.2, a desorption energy that is by 1 - 3 kJ/mol higher than that of the α_2 state, which dominates the emission in the 1.0 ML UP spectrum. If we assume a constant ΔE_{final} in the sub-monolayer range, than the direction of the shift is indeed in agreement with a binding contribution of the $1\pi_u$ orbital which is higher for α_3 than for α_2. However, the observed peak shift is much larger than ΔE_{des}, which is only 0.01 - 0.03 eV, and additional effects (e.g., more effective screening of α_2 compared to α_3) may play the major role.

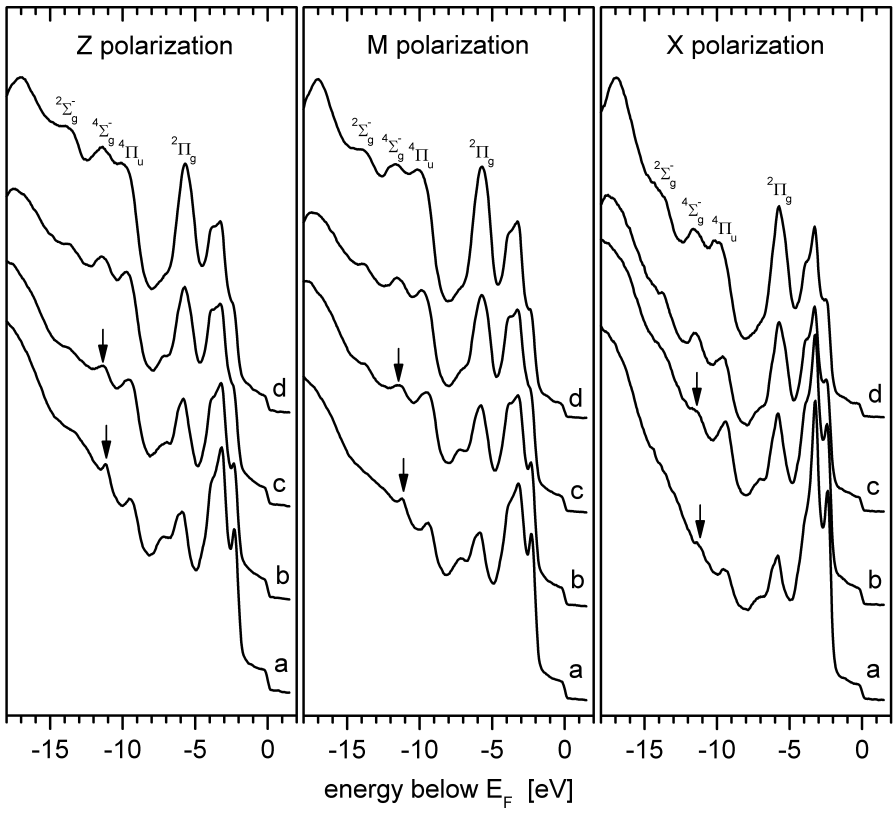

Fig. 5.6. Polarization-resolved UP spectra (hν = 24 eV) of physisorbed O_2 on Au(110)-(1×2). The incidence angle of the linearly polarized UV light was varied in the $(00\bar{1})$ mirror plane (with the polarization vector parallel to that plane). The photoelectrons were detected in normal emission ($\phi = 0°$). See Section 4.2.2 for the geometric details of the experiment. The spectra correspond to the following coverages: (a) 0.6 ML, (b) 1.2 ML, (c) 1.9 ML, (d) 2.5 ML. Sample bias –10 V as explained in Section 4.3.4. Significant changes in peak intensities are marked by arrows.

The changes in the region of the Au 5d band, especially between 2.0 and 4.0 eV below E_F, can also be induced by the adsorption of other gases on Au(110)-(1×2), namely, CO, CO_2, C_2H_4, H_2O, CH_3OH, or even Ar and Kr, as shown in the following chapters for some of these adsorbates. This observation suggests that most of the respective changes are not specific to oxygen adsorption. Instead, they are possibly due to a scattering of the photoelectrons on the adsorbed particles, as shown by Jacobi and Rotermund for several other adsorbate systems [Ja83]. A similar effect of adsorption on the d-band emission was reported for Ag(110) [Tj90]. Additionally, the incident UV radiation is partially absorbed by the adsorbate layer, which should also attenuate the d-band emissions.

Polarization-resolved UPS experiments (within the limitations described in Section 4.2.2) revealed, at the first glance, no significant dependence of the relative peak intensities on the polarization of the incident linearly polarized UV light. This holds especially for the multilayer range, as the UP spectra in Fig. 5.6 illustrate. However, a closer inspection of spectra for 0.6 ML and 1.2 ML shows that the levels of Σ symmetry (especially $^4\Sigma_g^-$) lose intensity, in contrast to those of Π symmetry, if the polarization turns from Z to X. This

means, according to the dipole selection rules, that the $3\sigma_g$ orbital has a preferential orientation normal to the surface, i.e., the molecules stand upright. The effect is only small, so that the molecules may as well be inclined to the surface. Clarification of this point would mainly require precise measurements, especially in the submonolayer range, with prolonged data acquisition in order to improve the signal to noise ratio. However, the danger of beam damage as described in Section 5.2.3 prevented the necessary extension of the measurement time. The curves in Fig. 5.6 represent the best compromise between an acceptable noise level on the one hand and the beginning formation of chemisorbed oxygen on the other.

coverage [ML]	$1\pi_g^* / {}^2\Pi_g$	$1\pi_u / {}^4\Pi_u$	$3\sigma_g / {}^4\Sigma_g^-$	$3\sigma_g / {}^2\Sigma_g^-$
0.25	≈ 5.4	9.6	≈ 11.2	≈ 13.6
1.0	≈ 5.4	9.4	11.2	13.6
8.8	5.9	10.1	11.7	14.1
vertical gas phase I.P. [Tu70]	12.3	16.7	18.2	20.4
I.P. - ($\varphi + \Delta\varphi$)	7.2	11.6	13.1	15.3
$\Delta E_{final} + \Delta E_{initial}$ for 1.0 ML	1.8	2.2	1.9	1.7
$\Delta E_{final} + \Delta E_{initial}$ for 8.8 ML	1.3	1.5	1.4	1.2
E_i(8.8 ML) - E_i(1.0 ML)	0.5	0.7	0.5	0.5

Table 5.2: Peak positions (in eV, ± 0.1 eV) of the valence levels of physisorbed O_2 on Au(110)-(1×2). The peaks are classified by the molecular orbital from which the photoelectron was ejected and by the corresponding final state of the molecular ion[8]. The energy scales were aligned by subtracting the difference between E_F and E_{vac}, $\varphi + \Delta\varphi$, from the vertical gas phase ionization potentials (values of the latter after [Tu70]). $\Delta E_{final} + \Delta E_{initial}$ denotes the difference between the corrected gas phase I.P. and the respective peak position in the adsorbate spectrum. For the meaning of ΔE_{final} and $\Delta E_{initial}$ cf. Section 4.2.1.

Physisorbed oxygen layers with a preferential orientation of the molecules perpendicular to the surface have also been found on graphite (0001). Apart from the δ phase with lying molecules (molecular axis parallel to the surface) an antiferromagnetic ε phase and a paramagnetic ξ phase in which the molecule axis has a substantial contribution normal to the surface have been described [Gu92, Ro89, Pa88]. On other substrates, e.g., Pt(111) [Ou87, Pu95] and Ag(110) [Ou87, Pr86, Gu92a], the O-O axis is parallel to the surface.

[8] Strictly speaking, this classification by the irreducible representations of the point group $D_{\infty h}$ applies only for the isolated molecule. As usual in the case of weakly bound adsorbates, we tacitly ignored the reduction of the symmetry by the presence of the surface.

An ARUPS experiment did not show any dispersion of the O_2 valence states, nor were additional reflexes observed in a LEED experiment[9]. Thus, the physisorbed dioxygen does not form any structure with long-range order under the conditions of our experiments.

5.1.3. Work function change

Oxygen adsorption on gold causes a work function decrease, as it is generally observed in the case of physisorptive bonding. The respective $\Delta\varphi(\Theta)$ curve is displayed in Fig. 5.7. At monolayer coverage (corresponding to an exposure of 2.6 L) the curve reaches a minimum (-0.22 eV) which is not specific to our system. For a comparison with literature data, the first adlayer of physisorbed dioxygen on O/W(110) caused a work function decrease of 0.35 eV [Le76]. A work function minimum was also found for dioxygen physisorbed on Al(111) [Ho79] and for numerous other physisorption systems.

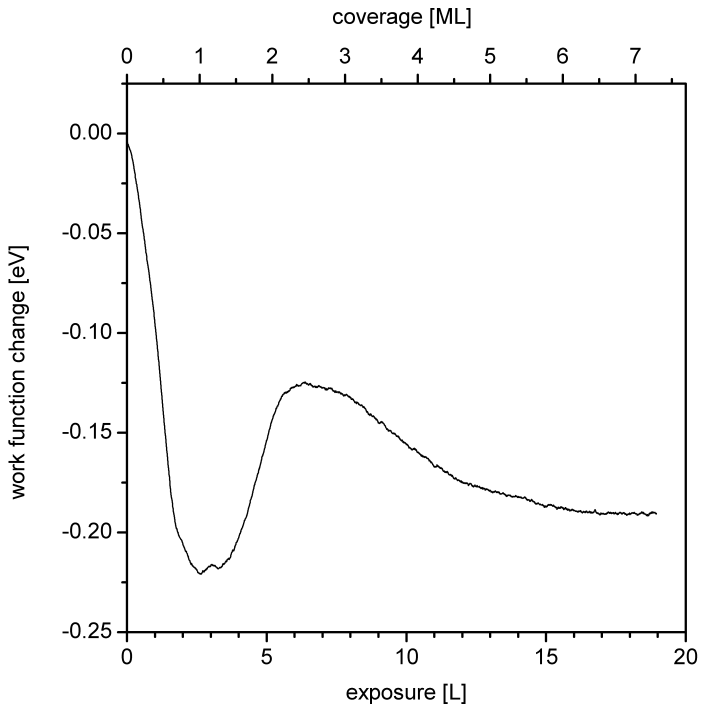

Fig. 5.7. Work function change variation induced by O_2 adsorption on Au(110)-(1×2) at 28 K. O_2 partial pressure 2×10^{-8} mbar. For the experimental details of the work function measurement, see Section 4.3.4.

[9] It should be mentioned that all LEED experiments, even those with lowest beam intensities, caused measurable damage on the adsorbate resulting in the formation of chemisorbed oxygen.

Higher O_2 coverages lead first to a work function increase, but after a maximum at 2.5 ML (6.4 L), corresponding to a $\Delta\varphi$ value of - 0.125 eV, the curve approaches a saturation limit of - 0.18 eV and remains constant above ≈ 7 ML (≈ 18 L).

Low UV beam intensities were always used in order to avoid beam damage of the adsorbate. To confirm that chemisorbed oxygen was neither spontaneously formed nor due to the influence of the UV irradiation, the sample was heated to 70 K after the measurement. This heating step completely restored the initial work function value of the clean surface. As shown in Section 5.2.3, formation of chemisorbed oxygen species leads to a work function increase. The chemisorbed oxygen desorbs only above 500 K. We conclude that the conditions applied here allowed measurements on an undamaged adsorbate layer.

Below 0.6 ML, the work function depends almost linearly on coverage. Thus, the Helmholtz equation (Eq. 4.48) can be applied in this range to determine the initial dipole moment, μ_0, of the individual adsorption complex. With an absolute coverage of $\sigma = (3.1 \pm 0.6)\times10^{18}$ oxygen molecules per m^2 corresponding to $\Theta = 0.6$ ML, an absolute value of $|\mu_0| = (0.20 \pm 0.4)$ D was obtained for the initial dipole moment.

5.1.4. NEXAFS measurements

A representative set of NEXAFS spectra of physisorbed dioxygen is displayed in Fig. 5.8. The spectra were taken at 28 K for normal beam incidence. Normalization with respect to the coverages leads to the decreasing noise level at constant signal intensity for increasing coverages.

The spectra show an intense π^* resonance at 530.9 eV due to excitation into the half-occupied O_2 $1\pi_g^*$ orbital and a split σ^* resonance with the two signals shifting around 539.8-540.0 eV and 542.2-543.4 eV. In the respective literature, the σ^* double structure had originally been assigned to the two final states of different spin ($^4\Sigma_g^-$ and $^2\Sigma_g^-$) connected with the excitation into the O_2 $3\sigma_u^*$ orbital [Wu90, St92]. More recently, this assignment was questioned by Karis et al., who claimed, in a combined theoretical and experimental (XPS, UPS, NEXAFS) study, that the split resonance is due to excitation into Rydberg states of different symmetry [Ka96]. Their (somewhat vague) argument is that the paramagnetic splitting in O_2 does, according to XPS and UPS measurements on the 1s and the $3\sigma_g$ orbital, respectively, not change upon physisorption[10], whereas the σ^* splitting in NEXAFS depends on whether the molecule is in the gas phase or in a physisorbed state. Furthermore, the paramagnetic splitting found with XPS and UPS is generally smaller (between 1.15 eV and 2.2 eV) than that observed with NEXAFS (3-4 eV). According to another interpretation, supported by DES[11] experiments which showed a par-

[10] In our experiments described in Section 5.1.2, we found a small difference of 0.2 eV between the splitting in physisorbed or condensed O_2 (2.4 eV, see Table 5.2) and that in the gas phase molecule (2.2 eV [Tu70]).

[11] Deexcitation Electron Spectroscopy

amagnetic splitting of only 0.6 eV for the 1s → $3\sigma_u$* transition, only the first of the two signals is due to excitation into the O_2 $3\sigma_u$* orbital, whereas the second signal appearing at higher photon energy is due to transitions into Rydberg orbitals [Ne93]. Our spectra support both of the more recent interpretations. Firstly, they confirm a dependence of the σ* splitting on the local environment of the O_2 molecule. Secondly, they show that the position of the peak at higher photon energy, σ_2^*, varies indeed much more than that of the other peak, σ_1^* (Table 5.3).

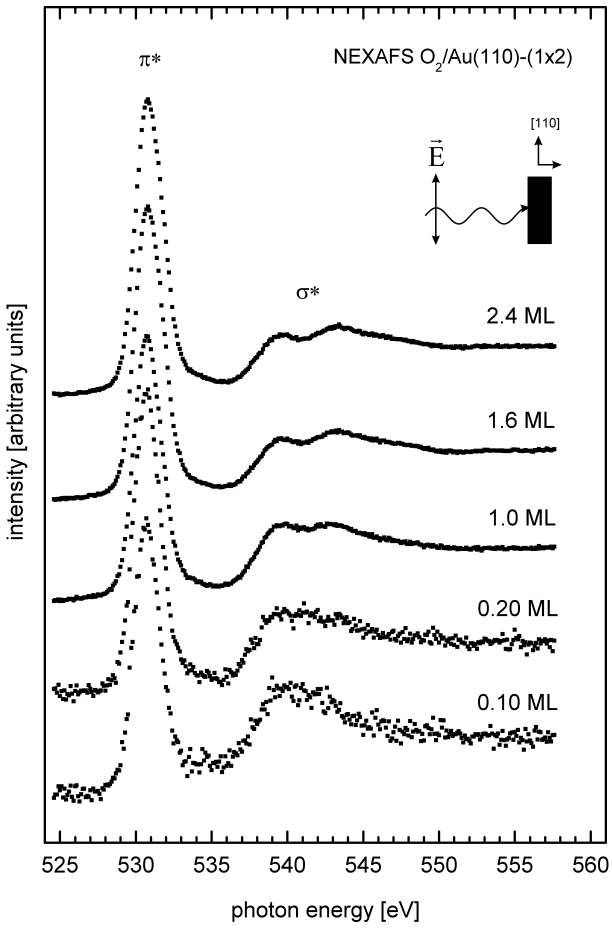

Fig. 5.8. NEXAFS spectra of physisorbed dioxygen on Au(110)-(1×2) at 28 K. An exposure of 2.6 L was applied to obtain monolayer coverage. The beam incidence was normal to the surface, and the polarization vector was parallel to the [$\bar{1}$10] direction, i.e., to the trenches of the reconstructed (110) surface. The spectra are corrected for differences in the photon flux and normalized with respect to the coverages, but not normalized to the step between the onset of the π* resonance and the continuum. See text for the details.

These assignment problems aside, we can state that all features in our NEXAFS spectra are almost identical to those observed on physisorbed dioxygen on Pt(111) [Wu90] and closely resemble the gas phase spectrum of O_2. Especially the position of the σ* resonance of adsorbed molecular oxygen compared to that of condensed oxygen gives information about the bonding state. In the case of chemisorbed O_2 on Pt(111), a red-shift of

≈ 5 eV (relative to condensed oxygen) was observed. For O_2 on Ag(110) [Ou87], the shift was even larger, ≈ 8 eV. The fact that the peak shift between submonolayer and multilayer coverages is much smaller, ≤ 1.2 eV, again excludes chemisorptive bonding contributions of dioxygen on Au(110)-(1×2).

Variation of the beam incidence angle parallel to the $(00\bar{1})$ plane (with the vector potential parallel to that plane) did not cause significant differential changes in the peak intensities. However, the identification of small effects would have required low-noise measurements with prolonged data acquisition, which, as in the case of UPS, caused the formation of intolerably high coverages of chemisorbed oxygen. This could be shown by subsequent TDS and Δφ measurements. We have reasons to assume that the photon beam and the secondary electrons also disturb a possible preferential orientation of the oxygen molecules on the surface, since this process requires far less energy than the irradiation-induced dissociation of the molecules, which is in detail described in the following section.

	Θ [ML]	$E(\sigma_1^*)$ [eV]	$E(\sigma_2^*)$[eV]	$E(\sigma_2^*) - E(\sigma_1^*)$ [eV]
	0.1	594.0	542.2	2.2
O_2/Au(110)-(1×2)	1.0	539.9	542.9	3.0
	2.4	539.8	543.4	3.6
variation with Θ		Δ = -0.2	Δ = 1.2	Δ = 1.4
gas phase [Ka96]		539.4	541.6	2.2

Tab. 5.3: Peak positions of the split σ* resonance for physisorbed O_2 on Au(110)-(1×2).

5.2. Activation of physisorbed molecular oxygen

5.2.1. Electron stimulated adsorption

Apart from physisorption, no spontaneous interaction of dioxygen with a Au(110)-(1×2) surface was observed. However, we found that physisorbed dioxygen adlayers are sensitive towards irradiation with low-energy electrons or UV photons: exposure to electrons with energies between 10 eV and 500 eV, or to UV-light in the range of 10 eV to 32 eV, induces the formation of chemisorbed oxygen.

Few examples exist in the literature in which it was shown that electron bombardment of a surface during exposure to O_2, but also to CO and CO_2, at room temperature causes a substantial increase in reactivity. On a polycrystalline nickel surface, the rate of oxidation could be increased by a factor of 5 if the surface was irradiated with electrons (850 eV, 150 μA) during exposure to molecular oxygen at room temperature [Ve76].

Electron bombardment of Ni(110) during exposure to CO led to the formation of nickel carbide up to several monolayers, whereas CO_2 caused oxidation of the surface under the same conditions [Ve79]. For effects of this type the terms 'electron enhanced adsorption' [Ve76] or 'electron stimulated adsorption' (ESA) [Li80] have been suggested.

Furthermore, it is well-known that electron bombardment of condensed molecular films induces chemical reactions in the media. Accordingly, it was shown that ozone is generated in multilayer films of molecular oxygen exposed to an electron beam with electron energies above 3.5 eV. The mechanism of the O_3 formation involves O atoms produced by dissociative electron attachment or dissociative electronic excitation of O_2, depending on the electron energy [La97]. Ozone, on the other hand, is able to deposit oxygen on metal surfaces [Sa98].

We used the very convenient technique to produce atomic oxygen by irradiation of a physisorbed O_2 layer with electrons or photons to extend our studies to chemisorbed oxygen species. The results will be reported in Chapter 6. In the present section we focus on experimental and physical details of the irradiation-induced processes. In order to generate chemisorbed oxygen we used mainly electron bombardment of physisorbed O_2. The results obtained by UV irradiation were similar, but an effective activation required beam intensities exceeding those attainable with a He discharge resonance lamp, which means that e.g. a synchrotron radiation source is needed. Furthermore, a homogeneous activation over the whole diameter of the sample (10 mm) is desirable, especially for quantitative TDS experiments. For this purpose, a homogeneous beam with at least the sample diameter is required. This requirement is much easier to fulfil for an electron than for a photon beam.

In the case of activation by UV radiation, direct photoprocesses as well as processes induced by photoelectrons may contribute to the activation in the oxygen adlayer. However, within the range of our experimental possibilities it is hard to distinguish between these two possibilities; we therefore refrained from embarking on this subject.

5.2.2. Activation by electron bombardment: variation of parameters

Dioxygen was adsorbed at a sample temperature of 28 K and a O_2 partial pressure of 2×10^{-8} mbar, as described in Section 5.1. The adlayers of physisorbed O_2 were then bombarded with electrons under normal incidence. In the experiments described below, parameters of the activation, including duration of bombardment, initial dioxygen coverage, and electron energy, were systematically varied.

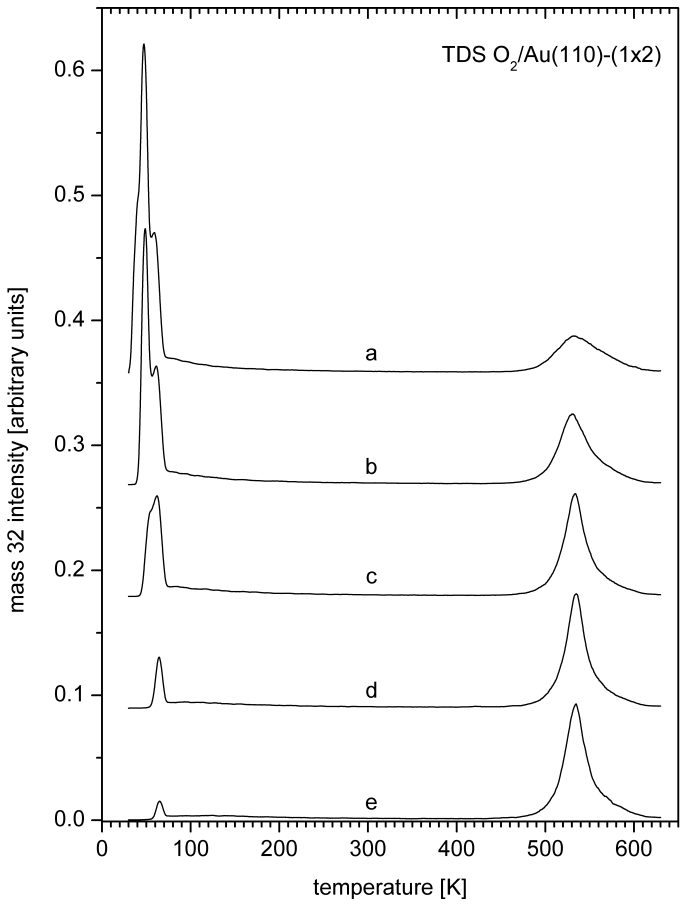

Fig. 5.9. Set of oxygen thermal desorption spectra (detected mass m/z = 32 amu, heating rate 2.35 K/s) measured after electron bombardment of 2.2 ML of physisorbed dioxygen at 28 K for increasing periods of time. An electron beam with 500 eV electron energy and a current density of 3.9 μA/cm^2 were applied. The desorption state above 500 K is attributed to chemisorbed oxygen generated by the electron bombardment; the low-temperature features belong to remaining physisorbed oxygen. Normalization by multiplication with $(T/K)^{1/2}$ as described in Section 4.1.6 was applied because of the large temperature range covered by the spectra. The spectra correspond to the following bombardment periods (in minutes): (a) 0.5; (b) 1.0; (c) 2.0; (d) 5.0; (e) 10.0.

VARIATION OF THE EXPOSURE TIME TO ELECTRONS AT FIXED ELECTRON ENERGY – The duration of the electron bombardment was varied for constant initial O_2 coverage of 2.2 ML and constant electron energy of 500 eV. The current density of the incident beam is not directly measurable. A *positive* current density of 1.5 μA/cm^2 was measured between the clean sample and ground, due to secondary electron emission that overcompensated the primary electron flux for primary electron energies above 150 eV. On clean gold, the secondary electron yield, defined as the ratio of emitted secondary to primary electrons, is 1.385 for a primary electron energy of 500 eV [La59]. Therefore, the primary electron current density in our experiment could be estimated to be 3.9 μA/cm^2, equivalent to 0.015 electrons per surface gold atom per second. The combined electron flux of primary and secondary electrons was 9.3 μA/cm^2, or 0.036 electrons per surface gold atom per second. However, the secondary electron yield will

change due to oxygen adsorption. This change would influence the total, but (of course) not the primary electron flux[12].

A representative set of oxygen thermal desorption spectra, measured subsequent to the bombardment at 28 K, is displayed in Fig. 5.9. Two main groups of signals can be clearly distinguished. The sharp desorption peaks of remaining physisorbed dioxygen appear between 35 K to 70 K, whereas the peak above 500 K is attributed to chemisorbed oxygen produced by electron stimulated adsorption. Additionally, low intensity oxygen desorption features occurred between 70 K and 150 K. For increasing periods of electron bombardment, the low-temperature peaks lose intensity, while the peak of chemisorbed oxygen grows until it reaches a maximum value (which is here *not* due to completion of a monolayer).

The thermal desorption spectra were integrated separately for the low-temperature (30 - 300 K) and the high-temperature (300 - 640 K) ranges. The resulting integrated intensities, which are proportional to the relative coverages of the respective species, are displayed in Fig. 5.10 as functions of the bombardment time. For the given conditions, nearly half of the initially adsorbed O_2 was removed by electron stimulated desorption, as indicated by the total coverage curve. The other half (> 40 %) was converted into chemisorbed oxygen after five minutes of electron bombardment, leading (in our example) to a coverage of chemisorbed oxygen of 0.70 (±0.14) oxygen atoms per gold atom. An exposure time of five minutes corresponded to a total charge of 11 electrons per gold atom. Therefore, about 20 electrons, primary and secondary, and ≈ 0.7 O_2 molecules were needed to produce one adsorbed oxygen atom.

On the gold surface covered with physisorbed *and* chemisorbed oxygen, a desorption maximum of physisorbed oxygen appears at 65 K, which corresponds to a desorption energy of ≈ 16 kJ/mol according to the Redhead formula with a 1st order frequency factor of $kT/h \approx 10^{12}\ s^{-1}$ ([Re62], see also Section 4.1.3). Comparison with the desorption energy of dioxygen adsorbed on clean gold (< 12 kJ/mol, see Fig. 5.2) reveals that the chemisorbed oxygen strengthened the physisorptive bond.

The question arises whether the TD signals below 70 K indeed reflect undissociated physisorbed oxygen and not any other oxygen species formed by electron bombardment. To clarify this point, we heated the sample after the activation to 200 K in order to completely remove the excess of physisorbed oxygen. After cooling to 28 K, oxygen was adsorbed onto the remaining chemisorbed oxygen, and the TD experiment was started without prior electron bombardment. This treatment led to identical low-temperature desorption features, a result that confirms the absence of any other desorbing oxygen species due to the bombardment.

[12] Alternatively, we biased the sample with a voltage just below E_{kin}/e_0 of the primary electrons in order to minimize the secondary electron yield. The resulting values for the primary current were slighly different from the indirectly determined, probably because the electric field around the sample due to a biasing influences the trajectories of the electrons and leads to wrong values for the beam current.

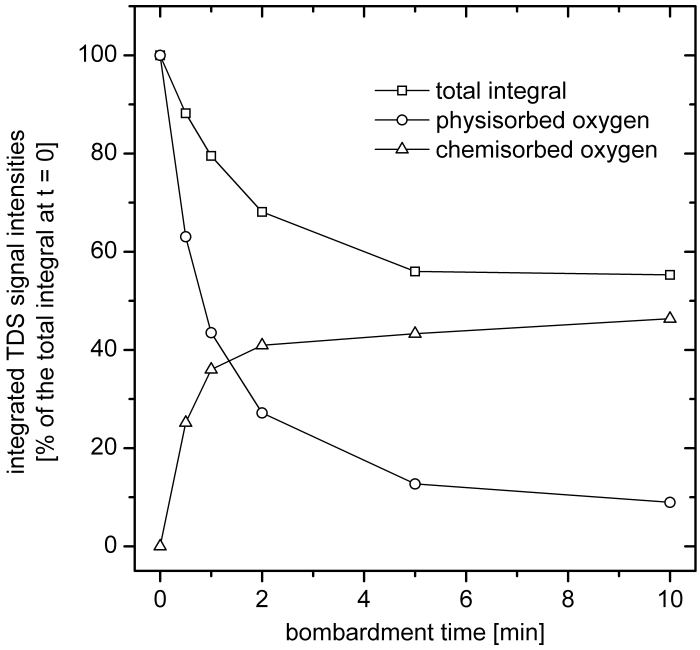

Fig. 5.10. Integrated TDS signal intensities of the spectra displayed in Fig. 5.9 in % of the total integral for the unbombarded physisorbed adlayer. The spectra were separately integrated between 30 K and 300 K ('physisorbed oxygen') and between 300 K and 640 K ('chemisorbed oxygen'). Nearly 50 % of the initially physisorbed dioxygen was converted into chemisorbed oxygen after a bombardment time of 10 min. For the conditions of the experiment, see Fig. 5.9.

VARIATION OF THE INITIAL O_2 COVERAGE AT FIXED ELECTRON ENERGY – In a second type of experiment, the initial O_2 coverage was varied at constant electron energy (500 eV) and duration of bombardment (3 minutes). The current density of the primary electron beam was again 3.9 $\mu A/cm^2$. Fig. 5.11 displays the absolute and relative coverages of chemisorbed oxygen vs. initial exposure and coverage of physisorbed dioxygen. The percentage of O_2 converted to chemisorbed oxygen (≈ 40 %) remains nearly constant for physisorbed O_2 coverages up to 5.9 ML (15 L), corresponding to a chemisorbed oxygen coverage of 1.0 ML (or 1.33 ± 0.27 oxygen atoms per gold atom) under the given conditions of activation (for the definition of the monolayer of chemisorbed oxygen see Section 6.1.1).

As the coverage of chemisorbed oxygen exceeds 1.0 ML, the activation process becomes increasingly inefficient. There are two possible reasons, both of which may apply. First, the gold surface is probably less reactive towards activated oxygen species after being saturated with a monolayer of chemisorbed oxygen, because the oxygen atoms, produced by electron bombardment, have to penetrate through a closed monolayer in order to occupy subsurface or bulk sites. Second, for the thicker dioxygen adlayers, the activation may take place too far away from the surface, thus preventing the activated species from reaching the surface before being deactivated. For example, oxygen atoms may recombine, or an ozone intermediate may be destroyed by electron impact before adsorption can

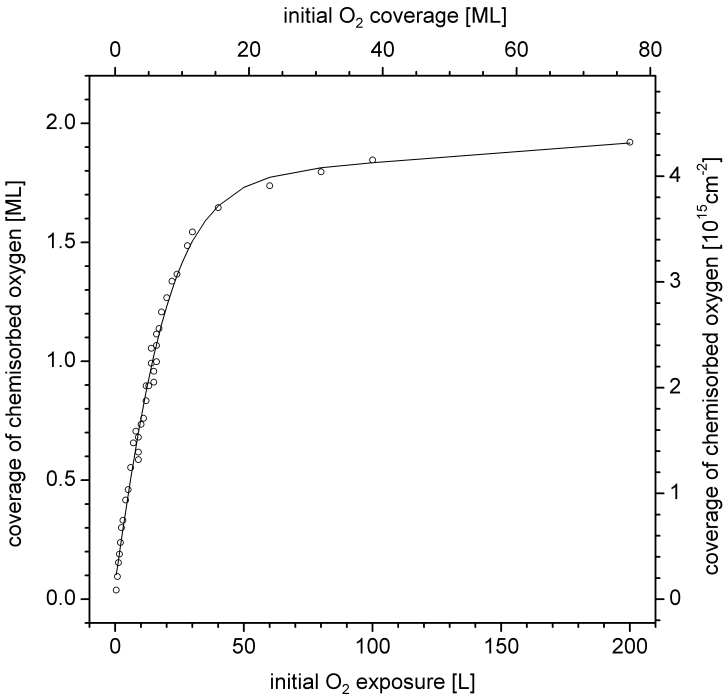

Fig. 5.11. Coverage of chemisorbed oxygen as a function of coverage (and exposure) of physisorbed dioxygen. The O_2 adlayers were bombarded for 3 minutes with an electron beam energy of 500 eV and a current density of 3.9 μA/cm^2. The coverages were obtained by integration of TD spectra in the range 300 – 650 K.

occur. As a result, thicker dioxygen adlayers favour electron stimulated desorption, a process which is always competing with the electron stimulated adsorption.

The question arises whether reactive, but relatively stable oxygen species such as ozone are formed during electron bombardment, species which may decompose upon heating and lead then to the oxidation of the gold surface. At low O_2 coverages (below 1.0 ML), the oxygen atoms generated by electron bombardment are likely to adsorb immediately on the surface. However, formation of ozone as an intermediate is expected for thicker films of molecular oxygen [La97]. Similar to gaseous ozone [Sa98, Pa90], the adsorbed O_3 molecule may supply oxygen atoms when it gets into contact with the surface after the thermal desorption of the remaining physisorbed O_2. The TD spectra measured after bombardment of thicker adlayers show O_2 desorption at temperatures between 70 K and 150 K (see Fig. 5.9). These signals might indicate ozone decomposition on the surface. However, we could not detect O_3 (m/z = 48) or an excess of O (m/z = 16, possibly formed by decomposition of O_3 by the ion source of the mass spectrometer) in the TDS experiments, nor did we observe emissions in UPS that could possibly be related to O_3. This apparent contradiction to the results of Lacombe et al. [La97] might be caused by the higher electron energies used in our experiment, leading to an ozone decomposition rate that exceeds the formation rate.

VARIATION OF THE ELECTRON ENERGY AT FIXED O_2 COVERAGE – Finally, the electron energy was varied at a constant initial O_2 coverage (2.2 ML) and for a constant duration of bombardment (5 minutes). Here arose the additional problem that the beam current of our electron gun changed significantly with electron energy. Apart from this problem, which made a quantitative analysis difficult, we found that the conversion of physisorbed into chemisorbed oxygen was generally accelerated with increasing electron energy. Therefore we used the highest electron energy available (500 eV) in most of the other experiments in order to keep the bombardment periods as short as possible.

However, the fact that the conversion rate increases with electron energy does not necessarily mean that high-energy electrons possess a higher cross section for activation. As shown by Lacombe et al. [La97], electron bombardment of condensed O_2 with electron energies above 3.5 eV leads to the formation of oxygen atoms due to dissociative electron attachment. At energies above 5.1 eV, i.e., above the O_2 dissociation energy, dissociative excitation is the main source of oxygen atoms. In the range of 3.5 to 10 eV, the efficiency of O atom production increases with electron energy and reaches a kind of plateau for higher energies. Therefore, it may be speculated that all electrons above the threshold of 3.5 eV are able to activate physisorbed oxygen, in other words, most of the secondary electrons contribute to the activation as well. The higher the energy of a primary electron, the more secondary electrons can be emitted on the surface (until the secondary electron yield decreases above a primary electron energy of 800 eV [La59]). The increased conversion rate at higher electron energies may therefore be caused by the growing number of secondary electrons possessing energies above the threshold value.

5.2.3. Beam damage

In the context of our UPS, $\Delta\varphi$, and NEXAFS measurements on physisorbed oxygen we already encountered the problem of damage[13] on a molecular adsorbate caused by an electron or photon beam. In the previous section, we systematically studied this effect as a technique for producing high coverages of chemisorbed oxygen. Now, we consider the extent of beam damage under the typical conditions of LEED or UPS measurements.

As an example, Fig. 5.12 shows the work function change during simultaneous O_2 adsorption and UV irradiation of the Au(110)-(1×2) surface at a sample temperature of 28 K. A value typical for UPS measurements at the beamline TGM 2 at BESSY-I was chosen for the beam intensity. The conditions were therefore similar to those applied during the work function measurement in Fig. 5.7, except for the higher photon energy (24 eV instead of 21.22 eV) and, above all, the much higher beam intensity (factor > 100). After an initial decrease, the work function reaches a minimum and then continu-

[13] 'Damage' refers to a process that converts physisorbed into chemisorbed oxygen, probably accompanied by the formation of reactive oxygen species like O, O_2^-, or O_3 as intermediates.

ously increases. Four minutes of irradiation lead to a work function increase of ≈ 0.5 eV relative to the value for the clean surface, indicating a coverage of chemisorbed oxygen of > 0.3 ML (see Section 6.5), if the competing parallel work function decrease due to physisorbed oxygen is neglected. For a LEED experiment with a typical beam intensity, the duration of exposure to the beam before substantial beam damage occurred was even shorter.

The irradiation of physisorbed O_2 leads also to substantial changes in the photoelectron spectrum. We irradiated 3 ML O_2 at 28 K with synchrotron light of the same intensity as applied for the $\Delta\varphi$ curve in Fig. 5.12. Thereafter, we heated the sample to 100 K in order to desorb remaining physisorbed oxygen and measured a UV photoelectron spectrum. If no beam damage occured, we would just find the spectrum of the clean surface. Instead, we obtained the spectrum displayed in Fig. 5.13 with additional intensity around 0 – 2 eV below E_F, which is, according to Section 6.4, indicative for the formation of chemisorbed atomic oxygen.

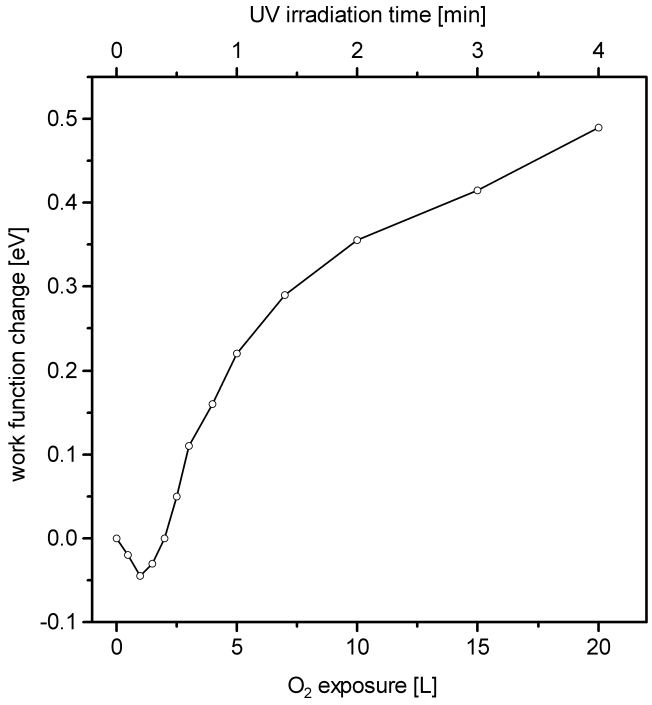

Fig. 5.12. Beam damage on physisorbed oxygen: work function change during simultaneous O_2 adsorption and UV irradiation of the Au(110)-(1×2) surface at a sample temperature of 28 K. Similar conditions as for the work function measurements in Fig. 5.7 were applied, except for the much higher beam intensity (factor > 100) and a slightly different photon energy (here 24 eV). The positive work function change is due to the formation of chemisorbed oxygen, a result that was confirmed by TDS and UPS (Fig. 5.13). Comparison with Fig. 5.7 reveals the dramatic beam damage on the adsorbate.

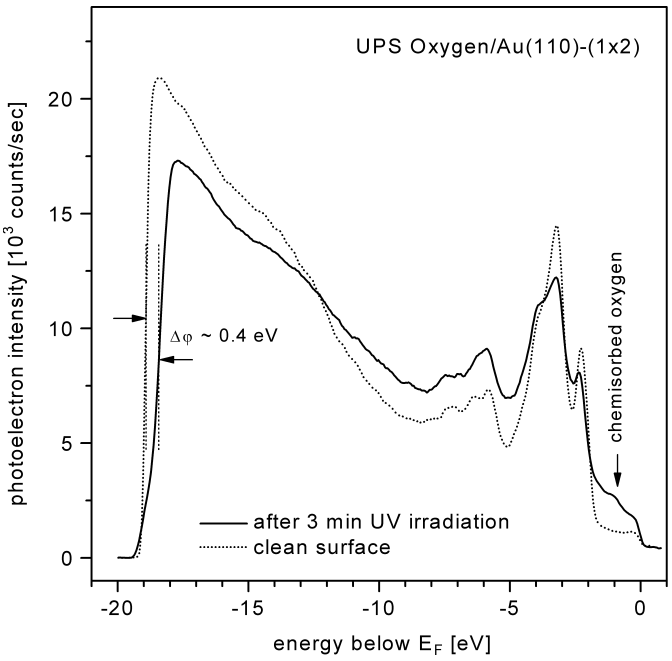

Fig. 5.13: UV photoelectron spectrum (24 eV, normal emission, M polarization) taken after 3 minutes UV irradiation of 3 ML physisorbed oxygen at 28 K and subsequent heating to 100 K (solid line). The spectrum was measured at a sample temperature of ≈ 100 K. For comparison, a spectrum of the clean surface at 100 K is shown (dotted line). The formation of chemisorbed oxygen is revealed by the work function increase and by the enhanced intensity right below E_F.

As an additional complication, the work function change due to the formation of chemisorbed oxygen also influences the UP signal positions of physisorbed oxygen, as illustrated in Fig. 5.14. One of the spectra (solid line) was measured immediately after dosing of 10 L (4 ML) oxygen at 28 K, the other one (dotted line) after 3 minutes irradiation (24 eV, same intensity as above). Clearly, the irradiation leads to a shift of all oxygen-induced emissions by 0.45 - 0.52 eV towards lower binding energies[14], a value which is similar to the work function increase of ≈ 0.44 eV caused by the chemisorbed oxygen. This shift reminds us of the fact that, in physisorption systems, the orbital energies are typically "pinned to the vacuum level (E_{vac})". A change in the work function is synonymous with a shift of E_F relative to E_{vac}. This in turn must lead to the observed shift of the O_2 levels relative to E_F. Our results are also reminicent of the "beautiful experiments[15]" by Jacobi and Rotermund [Ja82, Ro83], who measured (by UPS) the energy of the Ar $3p_{1/2}$ level relative to E_F on a substrate with varying work function. This work function variation was achieved by placing layers of molecules which cause different work function changes between a metal surface (Ni(110)) and the Ar layer, e.g., CO with $\Delta\varphi = +1.65$ eV or Xe with $\Delta\varphi = -1.0$ eV. The shifts of the Ar $3p_{1/2}$ peak followed ap-

[14] Except the $1\pi_u$ level, for which exact positioning is difficult.

[15] So described in Ref. [Er85], p. 124.

proximately the respective work function changes[16]. In our experiment, the substrate work function is changed *in situ* by generating a chemisorbed layer (underneath a physisorbed species) on the substrate under the influence of the UV irradiation. Unfortunately, this effect complicated also the precise UV spectroscopic investigation of the O_2/Au adsorption system, which was described in Section 5.2.2.

Our observations show that all experiments on reactive systems using particles possessing sufficient energy to induce chemical reactions demand a careful control of the conditions. Otherwise misleading results due to beam damage are likely to occur.

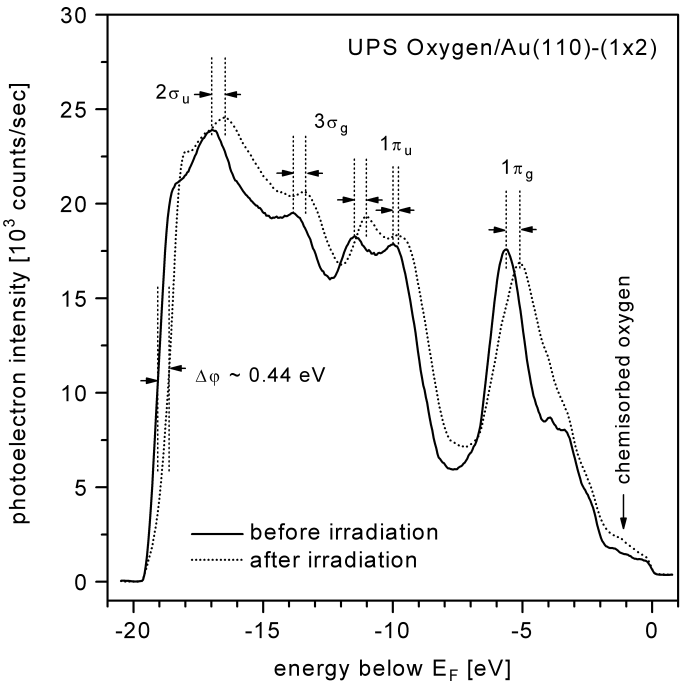

Fig. 5.14: UP spectra (24 eV, normal emission, M polarization) of physisorbed and condensed oxygen on Au(110)-(1×2). The solid line represents a spectrum measured directly after the adsorption of 4 ML oxygen at 28 K, the dotted curve was taken after 3 minutes irradiation with synchrotron light (24 eV). The peaks, except $1\pi_u$, shift by 0.48 – 0.52 eV toward lower binding energies, which is similar to the work function change of ≈ 0.44 eV. The smaller shift of the $1\pi_u$ level, 0.17 eV, may indicate that this level is less rigidly pinned to E_{vac}, because is interacts stronger with the surface. This, however, should only apply for the first layer. The formation of chemisorbed oxygen is also evident from the enhanced intensity at 0 – 2 eV below E_F.

[16] It should be mentioned that this interpretation has been controversially discussed. Especially the Eastman group propagated from 1980 onwards a different approach which explains the observed shifts by the different hole screening on the metal and in a matrix of condensed particles. A good introduction into the discussion is provided by Ref. [Ch86] and the references therein.